RI 9278

REPORT OF INVESTIGATIONS/1989

Effects of Al Additions on Sulfidation Resistance of Some Fe-Cr-Ni Alloys

By J. S. Dunning and S. C. Rhoads

BUREAU OF MINES

UNITED STATES DEPARTMENT OF THE INTERIOR

Mission: As the Nation's principal conservation agency, the Department of the Interior has responsibility for most of our nationally-owned public lands and natural and cultural resources. This includes fostering wise use of our land and water resources, protecting our fish and wildlife, preserving the environmental and cultural values of our national parks and historical places, and providing for the enjoyment of life through outdoor recreation. The Department assesses our energy and mineral resources and works to assure that their development is in the best interests of all our people. The Department also promotes the goals of the Take Pride in America campaign by encouraging stewardship and citizen responsibility for the public lands and promoting citizen participation in their care. The Department also has a major responsibility for American Indian reservation communities and for people who live in Island Territories under U.S. Administration.

Report of Investigations 9278

Effects of Al Additions on Sulfidation Resistance of Some Fe-Cr-Ni Alloys

By J. S. Dunning and S. C. Rhoads

UNITED STATES DEPARTMENT OF THE INTERIOR
Manuel Lujan, Jr., Secretary

BUREAU OF MINES
T S Ary, Director

Library of Congress Cataloging in Publication Data:

Dunning, J. S.

Effects of Al additions on sulfidation resistance of some Fe-Cr-Ni alloys / by J. S. Dunning and S. C. Rhoads.

(Report of investigations; 9278)

Bibliography: p. 19

Supt. of Docs. no.: I 2823:9278.

1. Chromium-iron-nickel alloys–Corrosion. 2. Chromium-iron-nickel alloys–Additives. 3. Aluminum. I. Rhoads, S. C. II. Title. III. Series: Report of investigations (United States. Bureau of Mines); 9278.

TN23.U43 [TN693.17] 622 s–dc20 [620.1'723] 89-600157

CONTENTS

ILLUSTRATIONS

TABLES

UNIT OF MEASURE ABBREVIATIONS USED IN THIS REPORT

°C	degree Celsius	mg	milligram
cm^3/min	cubic centimeter per minute	mm	millimeter
°F	degree Fahrenheit	μm	micrometer
g	gram	mpy	mil per year
h	hour	nA	nanoampere
in	inch	pct	percent
in^2	square inch	wt pct	weight percent
kV	kilovolt		

EFFECTS OF Al ADDITIONS ON SULFIDATION RESISTANCE OF SOME FE-CR-NI ALLOYS

By J. S. Dunning[1] and S. C. Rhoads[2]

ABSTRACT

The objective of this research by the U.S. Bureau of Mines was to determine the effects of Al additions on the sulfidation resistance of Fe-Cr-Ni alloys. A series of Fe-Cr-Ni alloys with and without additions of 4 pct Al were tested in a wet S vapor atmosphere at 677° C. A study of the morphology and composition of corrosion scales indicated a different corrosion mechanism for Al-free alloys compared with Al-containing alloys. Aluminum-containing alloys formed a compact, tightly adherent layer at the metal-scale interface that reduced corrosion rates by a factor of 3 to 10 compared with that of Al-free alloys. The thin, adherent Al-containing scale limited inward diffusion of O and S to the base metal and outward diffusion of Ni from the base metal.

Aluminum-containing alloys formed a three-layer scale in oxidizing-S environments, while Al-free alloys formed a less protective two-layer scale.

[1]Supervisory metallurgist.
[2]Research chemist.
Albany Research Center, U.S. Bureau of Mines, Albany, OR.

INTRODUCTION

Iron-base alloys, particularly Fe-Cr-Ni alloys, are construction materials for chemical processing vessels, pollution control equipment, coal gasifiers, and other equipment designed to operate above 500° C. In many instances, corrosive gases containing O and/or S are present. Under conditions of oxidation and/or sulfidation, the equipment often has a limited service life. Also, it is often necessary to use substantial amounts of Cr in the Fe-Cr-Ni alloys to achieve reasonable performance. In the metals industry, high-S environments are common in the processing of sulfide ores. In many situations, productivity, efficiency, and the economics of the process are materials limited because of temperature limitations imposed by severe corrosion, inherent in high-S environments.

As part of its program to develop technology to reduce the Nation's dependence on foreign sources of critical and strategic materials, the U.S. Bureau of Mines investigated the effects of Al additions on the sulfidation resistance of Fe-Cr-Ni alloys. Accordingly, one objective of this research is to understand the mechanisms of sulfidation occurring in Fe-Ni-Cr alloys, specifically the role Al plays in improving sulfidation resistance in oxidizing-S environments. A second objective is to reduce the amount of Cr required in Fe-base alloys in order to resist S-containing environments and to extend the service life of high-Cr-containing alloys in these environments, thereby conserving Cr. The most significant conservation of Cr would result from the alloy's extended service life if sulfidation rates could be reduced. Losses incurred through S corrosion are appreciable, and materials available for combating it are not considered adequate (*1*).[3]

The effect of adding Al to steels in order to improve their resistance against oxidation is well known (*2-6*). Aluminum also appears to be beneficial for alloys intended for use at high temperature in S, H_2S, and SO_2 atmospheres (*7-8*). However, while the corrosion mechanisms of Fe-Cr-Al alloys by O are relatively well known, this is not the case for corrosion by S, and S compounds. Mrowec (*9*) studied the corrosion of alloys with various Cr (18 to 25 pct) and Al (1 to 5 pct) contents in S vapor at atmospheric pressure, and Jallouli (*10*) studied alloys with 17 pct Cr and various Al (4 to 6 pct) contents under low-S vapor pressure. Both researchers observed the formation of a two-layer scale. The outer layer was noncompact and porous and allowed ready ingress of S, and the scale growth depended largely on the composition of the inner scale and its protective nature. Corrosion resistance in Al-containing alloys with the two-layer scale was not significantly increased.

The Bureau's research on the corrosion resistance of Al-containing stainless steels (*11*) in S vapor showed that the corrosion resistance of both ferritic and austenitic alloys improved with increasing Cr and Al contents. It was also observed that corrosion in wet S vapor (S vapor plus steam), which is an oxidizing environment, was less severe and the rates were less erratic than in dry S vapor, which is a reducing environment. To explain these empirical data, a series of Fe-base alloys with additions of Cr, Ni, and Al were prepared to study the role of these elements in providing resistance to S-containing environments. The performance of these alloys was compared with the performance of high-Cr AISI Type 310 stainless steel (Fe-25Cr-20Ni). This alloy is often specified for use in severe high-temperature corrosion environments and is acknowledged (*12*) as the best of the austenitic stainless steels for S vapor service to 704° C (1,300° F).

EXPERIMENTAL DESIGN AND PROCEDURES

The sulfidation characteristics of four Fe-base alloys were studied. Alloy A (Fe-17Cr-9Ni-4Al) is a ferritic alloy where Al is held largely in the form of an NiAl precipitate dispersed in the ferritic Fe matrix. Alloy B (Fe-17Cr-4Al) has the Al addition entirely in solid solution in a ferritic matrix. The comparison between alloys A and B was interesting because, while their Al content is the same, the NiAl precipitates in alloy A provide excellent strength at elevated temperatures, and ductility is improved because less Al is present in solid solution in the ferritic matrix (*13*). Thus, alloy A provides an excellent combination of workability, room-temperature ductility, and elevated temperature mechanical properties, while alloy B shows little ductility or strength at high temperature. Alloy C (Fe-17Cr-9Ni) is Al-free and exhibits a mixed austenitic-martensitic microstructure. Alloys A, B, and C were compared with alloy D (Fe-25Cr-20Ni), the Al-free, high-Cr, and high-Ni austenitic Type 310 stainless steel typically used in industry in high-S environments.

Corrosion rates of the four alloys were compared in wet S vapor at 677° C (1,250° F). Corrosion tests in wet S vapor were conducted in a cylindrical high-silica glass test chamber about 36 in long by 2.25 in OD, shown in figure 1. Sulfur vapor was provided by an internal, 4-in-deep annular reservoir of S, which was heated by a separate furnace. The reservoir was heated to 400° C (400 mm vapor pressure). A condenser (upper part of the test chamber) was maintained at about 154° C to provide continuous condensing and refluxing of S. Helium saturated with water vapor at 80° to 90° C and flowing at about 20 cm^3/min was injected into the chamber through the steam generator to provide an atmosphere that was about one-third each S, steam, and He. A flow of He (50 cm^3/min) was maintained across the outlet of the test chamber to prevent air from entering. Specimens were hung on the inner sidewall of the S reservoir by glass rods. Specimen

[3]Italic numbers in parentheses refer to items in the list of references at the end of this report.

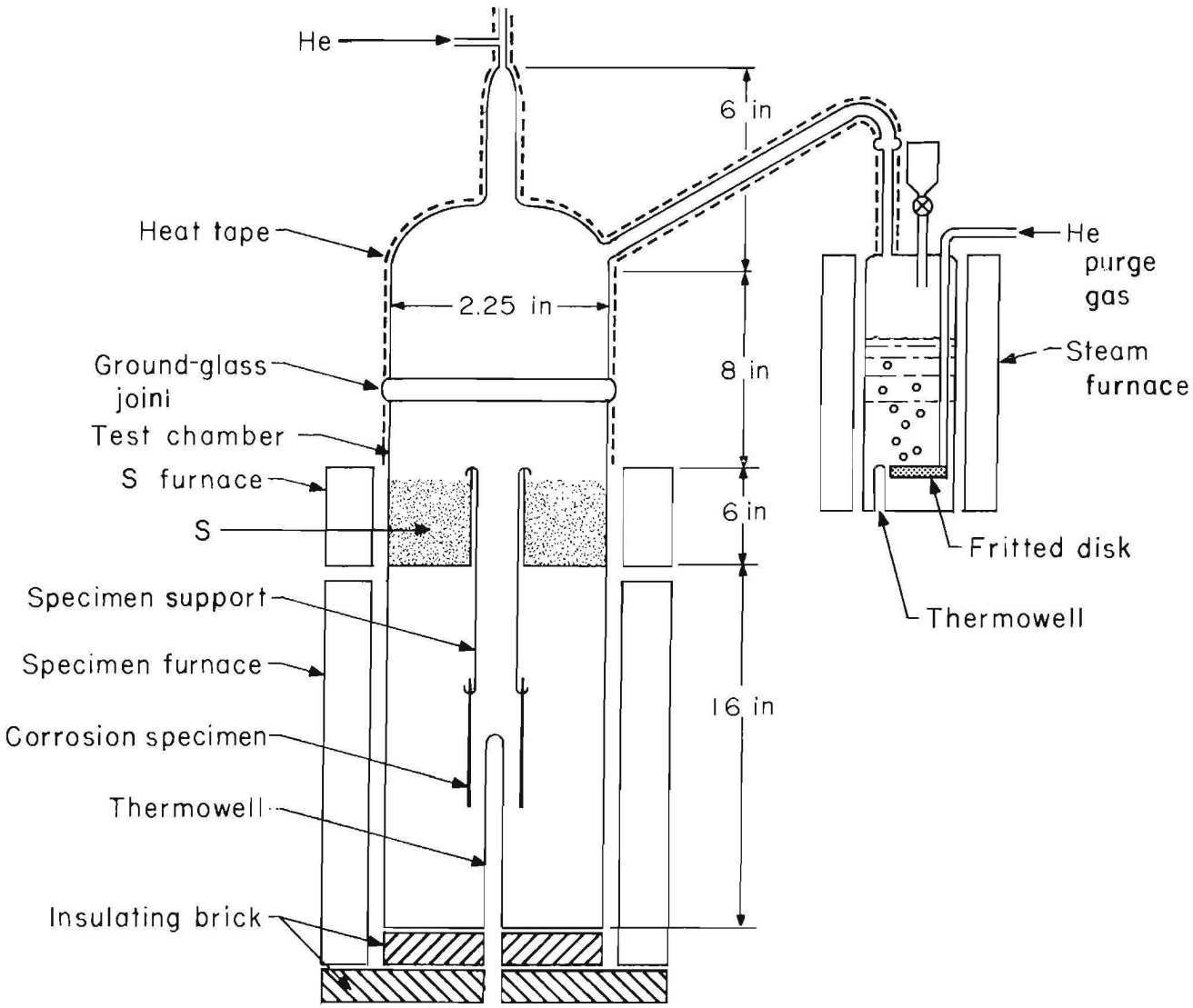

Figure 1.–Apparatus for laboratory corrosion tests in wet S vapor.

temperature was measured by a thermocouple inserted into a thermowell through the bottom of the test chamber. The thermowell extended to about the midpoint of the specimens. Temperature variation within the zone occupied by the specimens was held to ±10° C by external shunts on the furnace elements.

Duplicate specimens of each alloy were used in corrosion tests. One specimen was used for corrosion rate calculations, while the other specimen was used for metallography, scanning electron microscopy (SEM), and electron microprobe analysis (EMPA).

The specimens were approximately 1 by 1/2 in, and the surfaces were ground to a 120-grit finish. The specimens were cut from sheet rolled from 100-g ingots prepared by nonconsumable electrode arc melting. The ingots were prepared from electrolytic grades of Fe, Ni, and Cr, and high-purity Al. Standard Type 310 stainless steel was used as a standard for comparison purposes.

Corrosion rates were calculated from the initial surface area and the weight loss of descaled specimens. Corrosion products were loose and readily removed, except for an adherent, thin inner layer on Al-containing specimens, which was removed by vapor honing with a very fine grit waterborne sandblast. Vapor honing was carefully controlled to ensure minimal removal of base metal.

Specimens for metallography, SEM, and EMPA were removed from the test chamber and, after cooling in a desiccator, mounted in plastic epoxy resin. A small cross section was later cut from near the center using an abrasive cutoff wheel. Conventional metallographic mounting and polishing techniques were used, followed by electrolytic etching at room temperature in 10 pct oxalic acid.

Quantitative EMPA's were made on the polished surfaces of metallographic specimens using an electron microprobe equipped with three wavelength-dispersive spectrometers. Three elements were simultaneously

analyzed by measuring the intensities of the appropriate characteristic radiation. Operating conditions were 15 kV accelerating voltage and beam currents ranging from 30 to 150 nA.

The polished cross sections were also examined for elemental concentrations by SEM, energy dispersive analysis by X-ray (EDAX) elemental mappings, and point analysis.

RESULTS

The microstructures of the four test compositions are shown in figure 2. Alloy D was tested in the as-received austenitic condition, while alloys A, B, and C, after hot rolling at 1,100° C, were stabilized at the test temperature of 677° C for 24 h prior to testing. Alloy A has a fine dispersion of β-NiAl precipitates in a ferritic matrix. Analysis indicates approximately 50 pct of Al is in the form of β-NiAl. Alloy B shows a single-phase ferritic matrix with all the Al addition in solid solution, while alloy C exhibits a mixed austenitic-martensitic microstructure.

The specimens were held for 9 days (216 h) in wet S vapor at 677° C (1,250° F). (Data on corrosion rates are summarized in table 1.) The corrosion data confirmed earlier corrosion studies with similar compositions (*6*), indicating that the presence of Al in wet S vapor substantially reduces corrosion rates. Corrosion rates for alloy D were three to four times greater than the corrosion rates for the two test compositions with Al additions (alloys A and B). Corrosion rates for alloy C were approximately 10 times greater than the corrosion rates for alloys A and B. Corrosion rates for alloys A and B were not significantly different despite the fact that, in alloy A at 677° C, some Al is held out of solid solution in the form of a β-NiAl precipitate. The data agreed with prior corrosion studies of these types of alloys (*6*).

Table 1.–Corrosion rates of alloys after 9 days in wet S vapor at 677° C.

Alloy	Initial area, in^2	Weight loss, mg	Corrosion rate, mpy
A: Fe-17Cr-9Ni-4Al	0.491	67.9	43
B: Fe-17Cr-4Al	.552	66.1	37
C: Fe-17Cr-9Ni	.460	613.4	412
D: Fe-25Cr-20Ni	.567	283.6	154

One goal of this research was to study the corrosion films to determine why Al has this drastic effect on corrosion rates. Photomicrographs of the corrosion films on all four alloys are shown in figure 3. Thick scales were observed on the surfaces of the Al-free alloys; thinner scales were observed on the Al-containing alloys. In all four alloys, several layers could be observed in the corrosion films, including a very loosely adherent outer layer and a more adherent layer at the metal-scale interface.

An examination of the outer-scale surface revealed differences between the four alloys. Figure 4 shows photomicrographs of the outer-scale surfaces at a magnification of 50. All outer scales are porous and loosely adhered. The alloy C surface shows a coarse structure of large plate-shaped pyrrhotite (FeS) growths with habits of the low-symmetry NiAl structure. The outer layers on the other three alloys appear more uniform and compact at low magnification (fig. 4), but massive, dark, hexagonal crystals of FeS are visible on the surface of the Type 310 stainless steel, while the two alloys containing Al (alloys A and B) show bladelike plates of FeS that appear to be extruded from the surface of the scale. Higher magnification photomicrographs of the surface of alloys A and B are shown in figure 5. The surface on a finer scale appears very similar to that of alloy C. Isolated needles and elongated plate-shaped growths are evident, and the blades protruding from the surface are merely elongated, isolated platelets.

Further analysis of the corrosion products on the four alloys was conducted with the electron microprobe and energy dispersive X-ray. Quantitative identification of the phases present by X-ray diffraction was not possible because of the large number of stable sulfides and oxides possible in this system. While this has hampered the analysis of sulfidation specimens as compared with the analysis of oxidation specimens, considerable interpretation of the microprobe and X-ray data is possible. SEM profiles of the corrosion scale of all four alloys are shown in figure 6. Analyses of the scales are summarized in tables 2 through 5. Of major interest were the differences in scale composition between the Al-containing alloys (alloys A and B) and the Al-free alloys (alloys C and D).

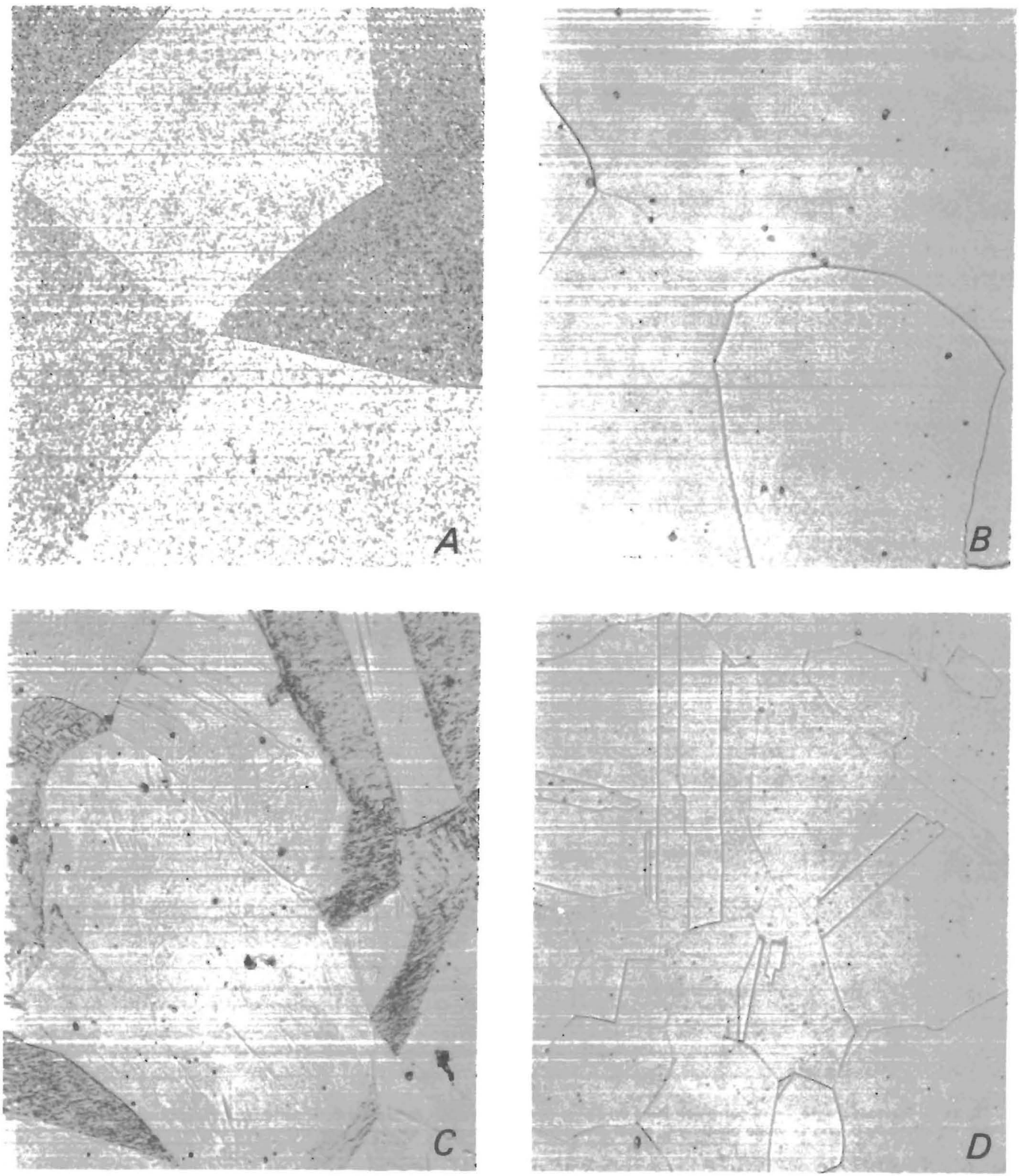

Figure 2.–Microstructures of alloys (X 500). *A*, **Alloy A;** *B*, **alloy B;** *C*, **alloy C;** *D*, **alloy D.**

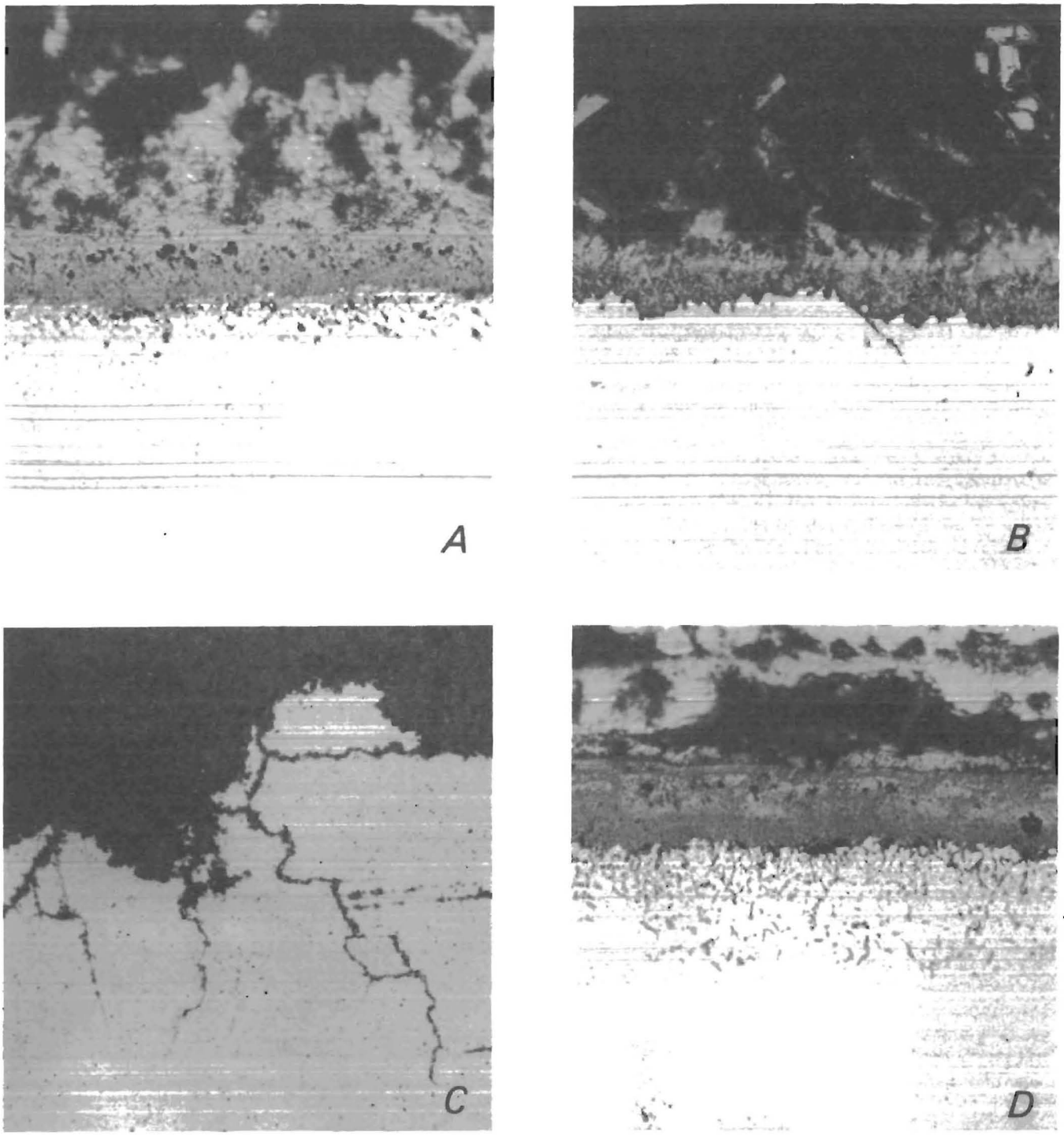

Figure 3.–Photomicrographs of corrosion films on alloys (X 400). *A*, Alloy A; *B*, alloy B; *C*, alloy C; *D*, alloy D. Complete films are shown on alloys A, B, and D, while on alloy C, inner one-third film and grain boundary sulfidation are shown.

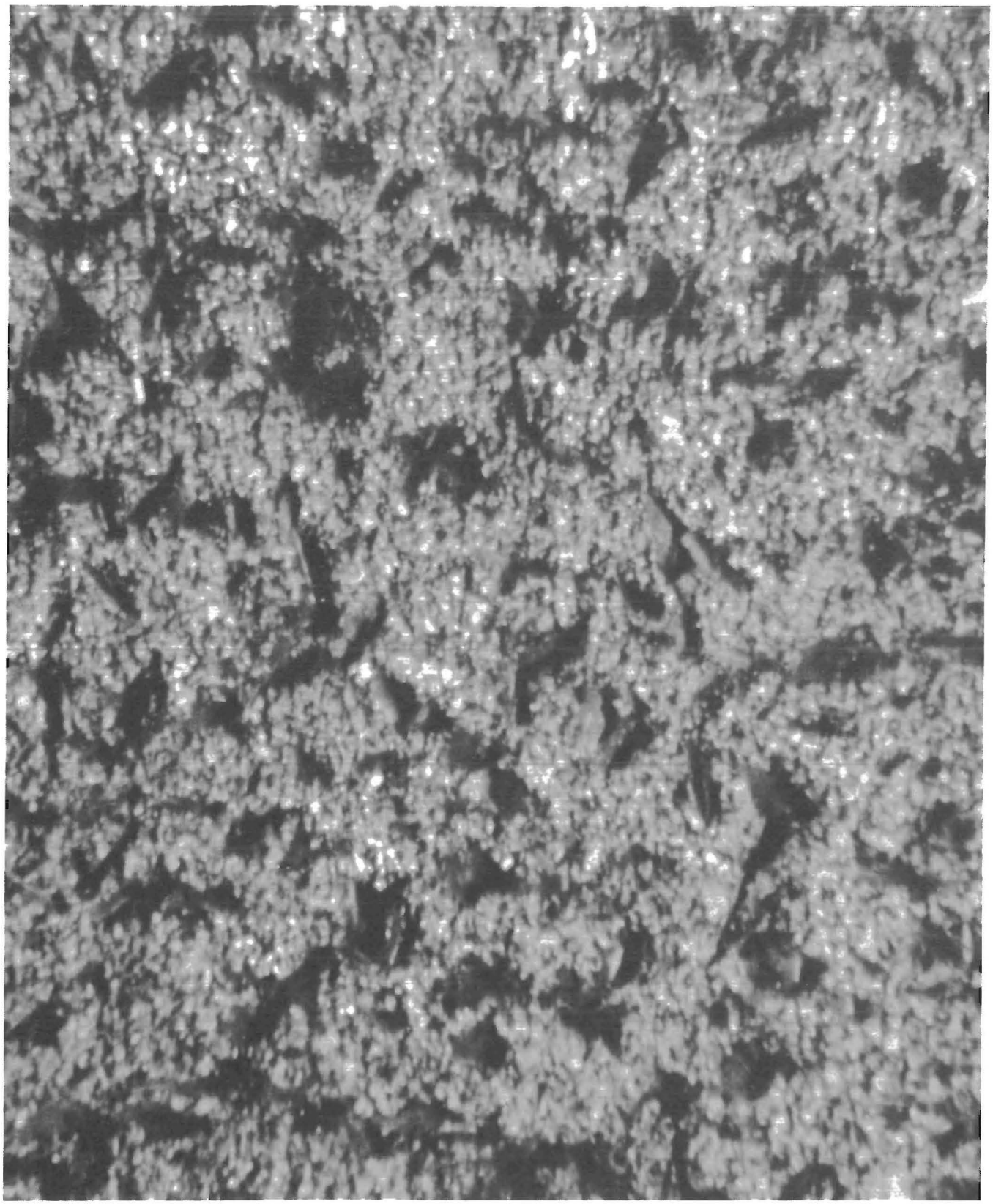

Figure 4.–Photomicrographs (X 50) of outer-scale surfaces of alloys–alloy A.

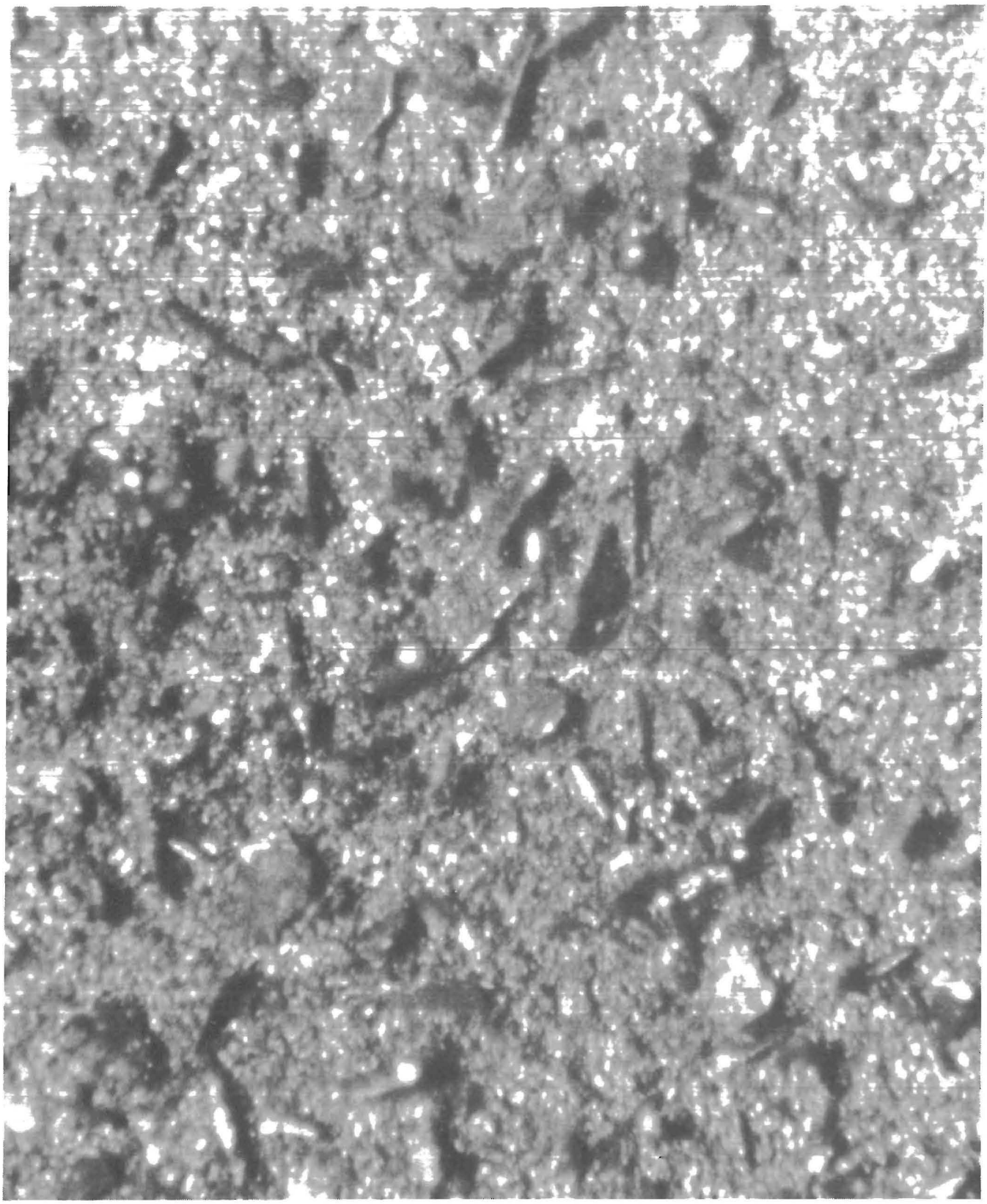

Figure 4.–Photomicrographs (X 50) of outer-scale surfaces of alloys–alloy B.

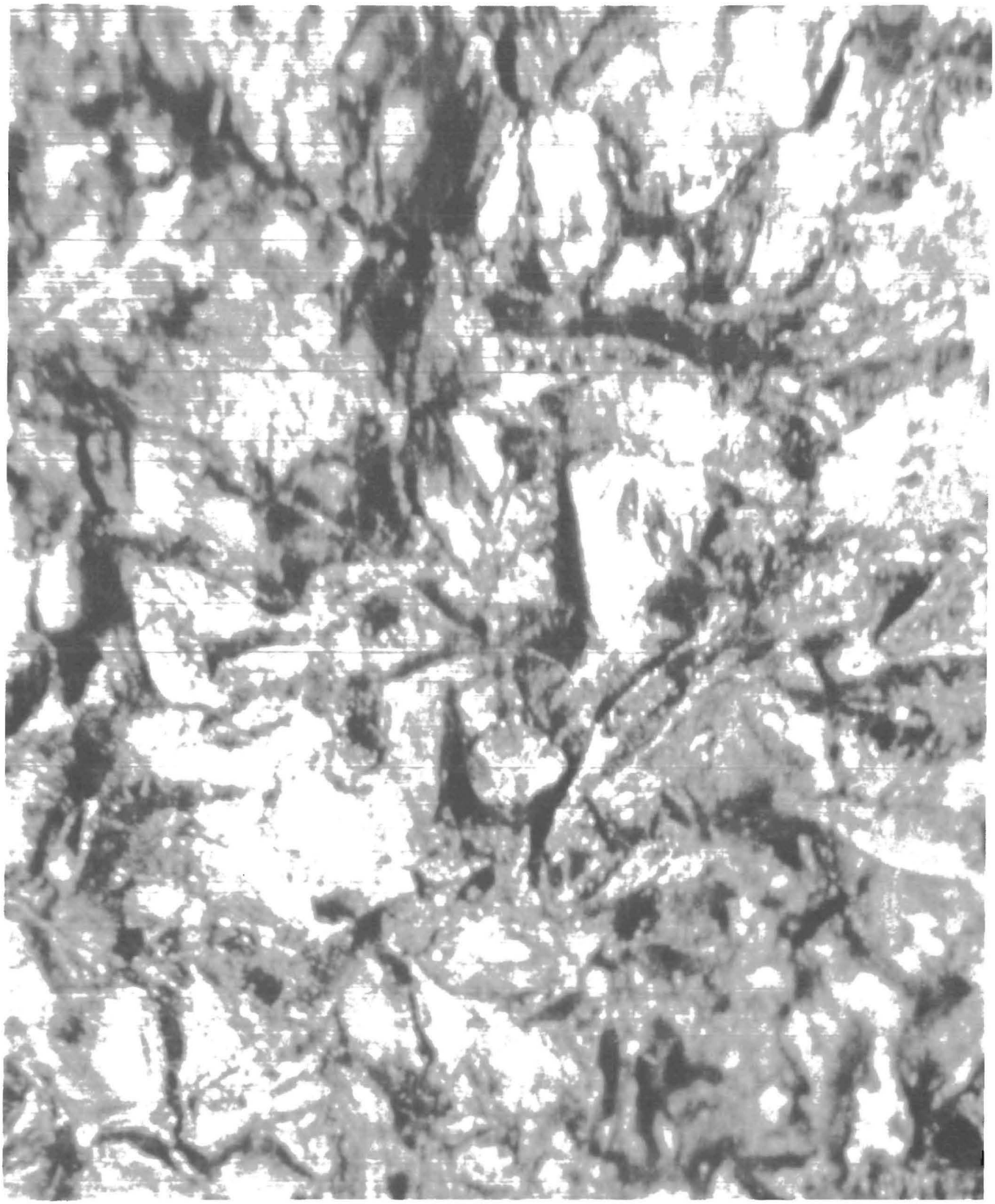

Figure 4.–Photomicrographs (X 50) of outer-scale surfaces of alloys–alloy C.

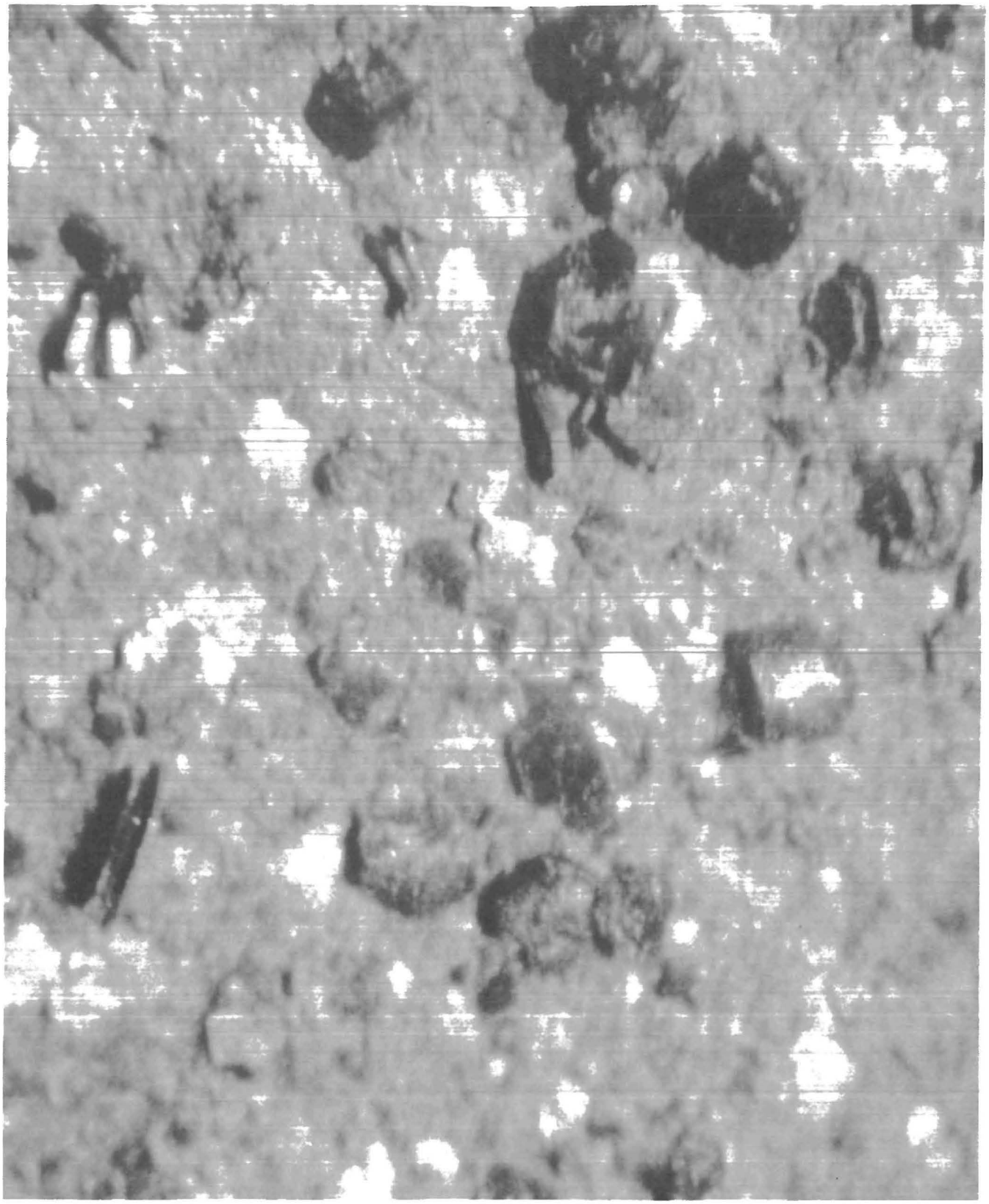

Figure 4.–Photomicrographs (X 50) of outer-scale surfaces of alloys–alloy D.

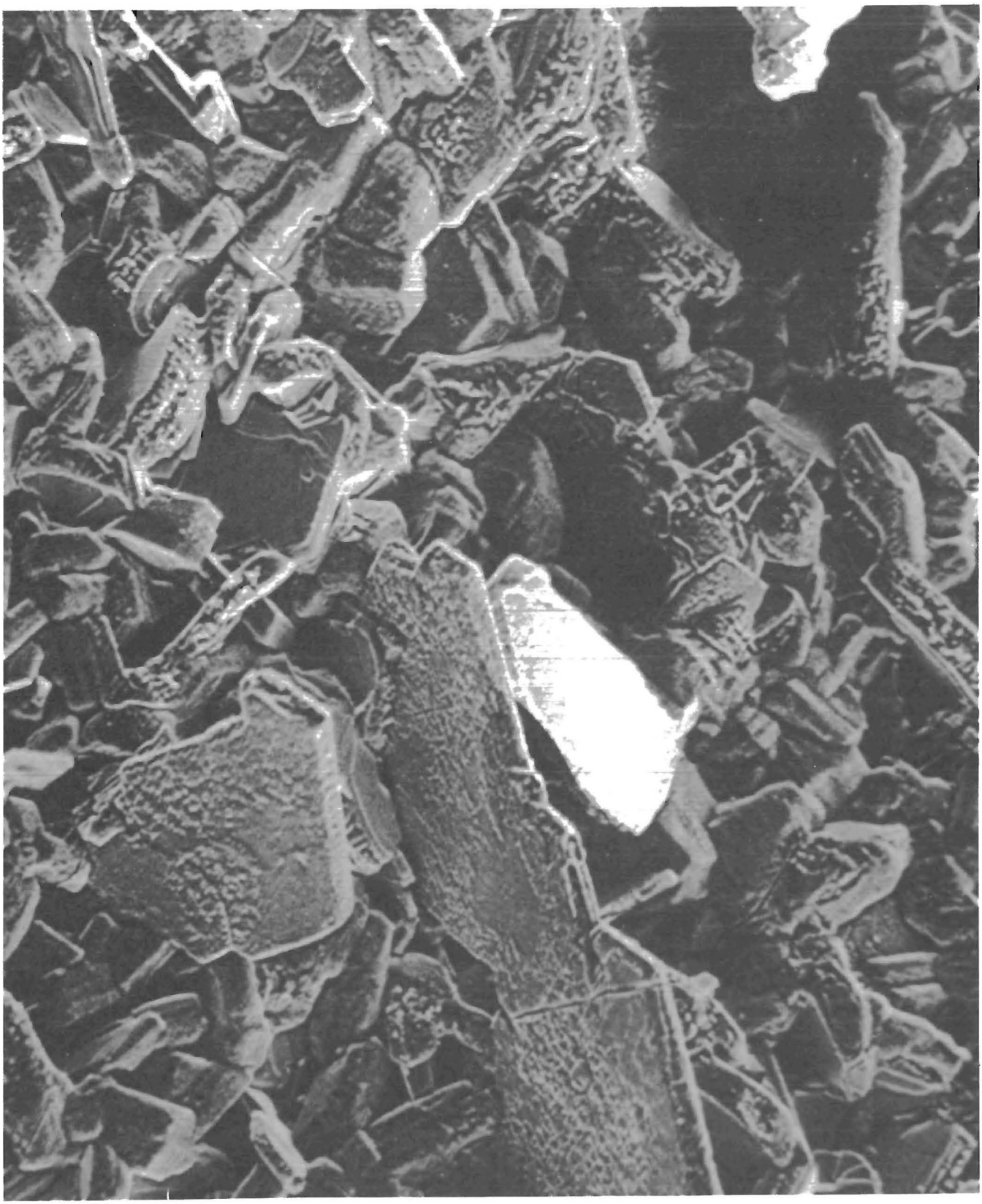

Figure 5.–Photomicrographs (X 250) of surfaces of alloys–alloy A.

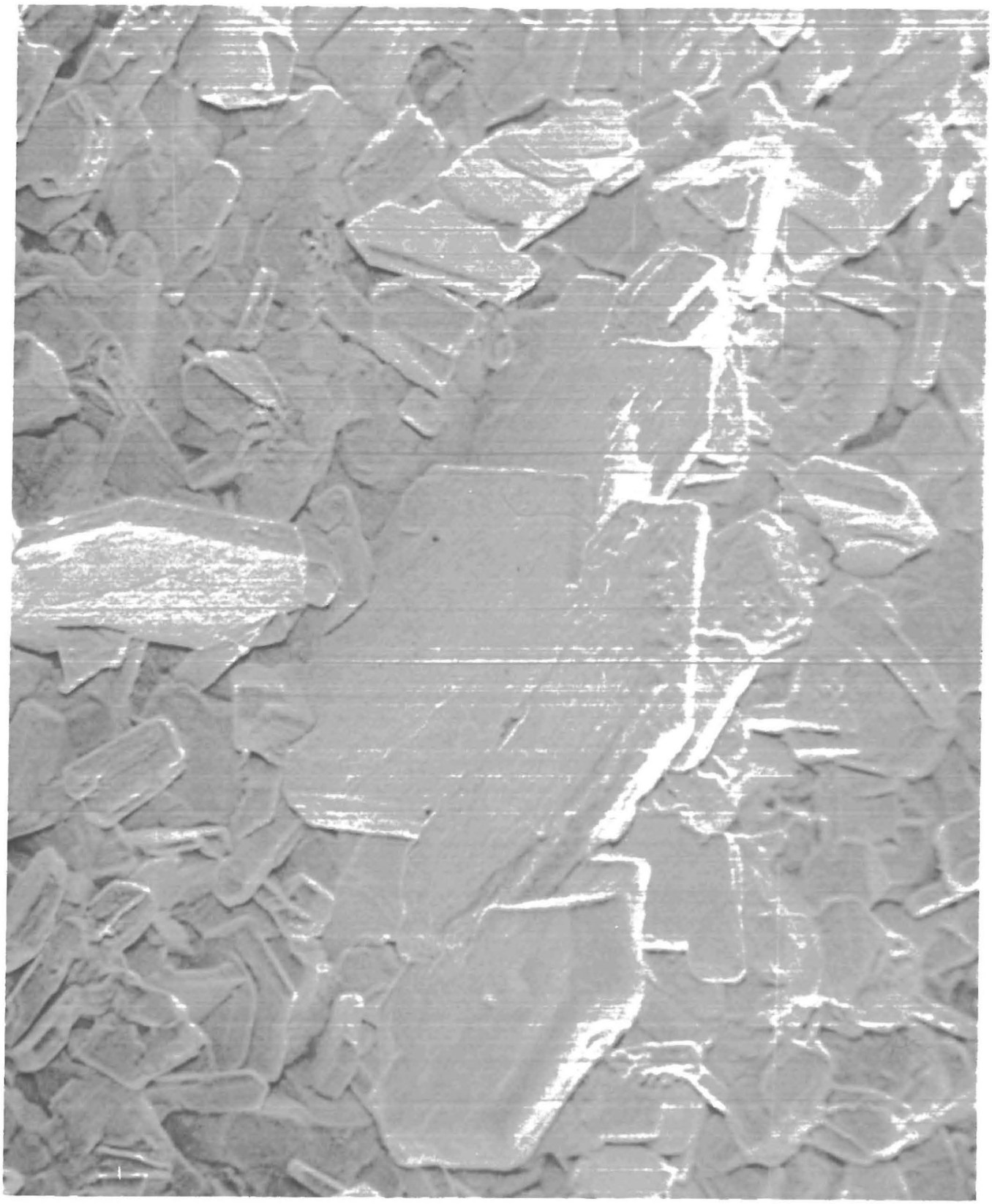

Figure 5.–Photomicrographs (X 250) of surfaces of alloys–alloy B.

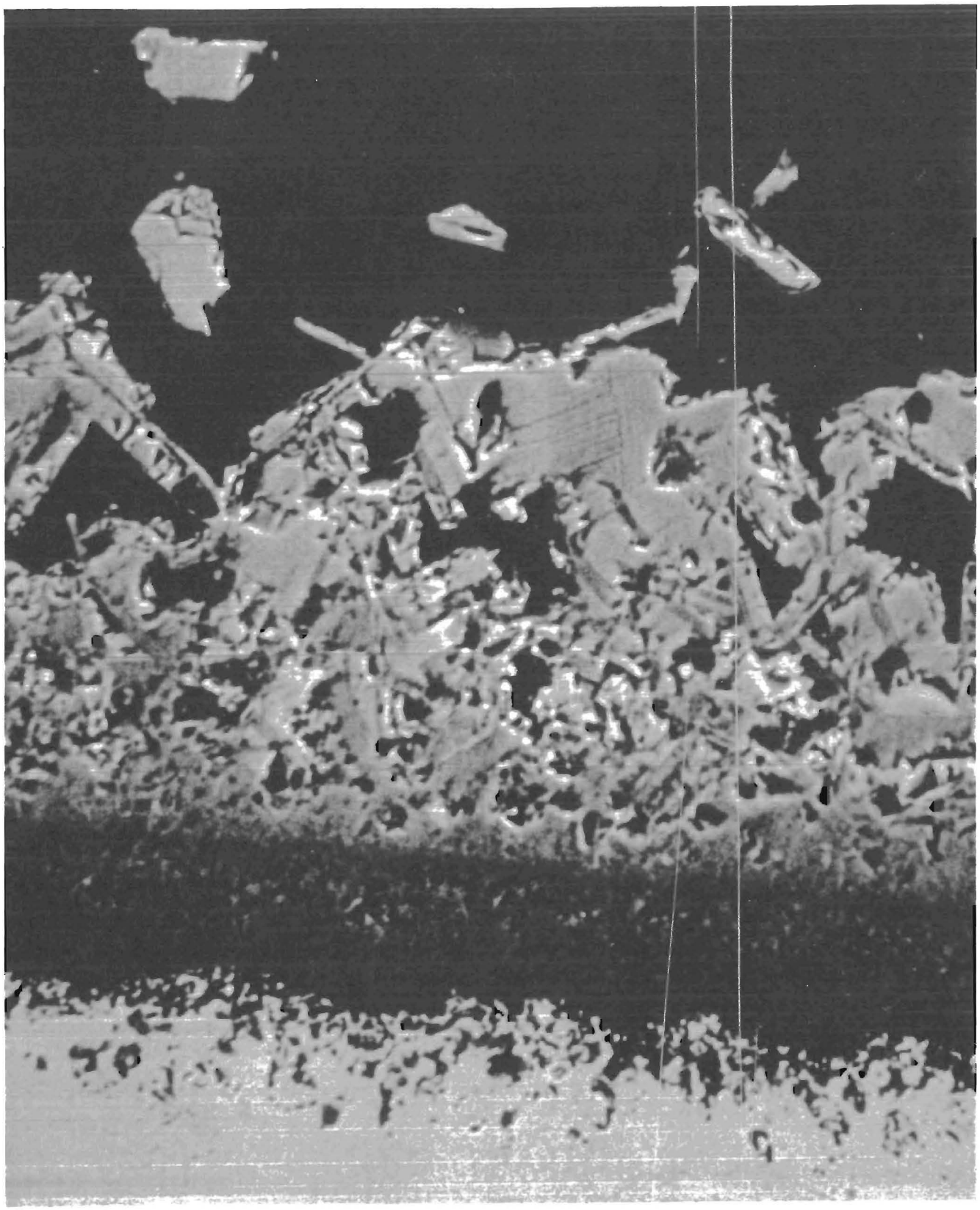

Figure 6.–Profiles of corrosion scales of alloys–alloy A (X 500).

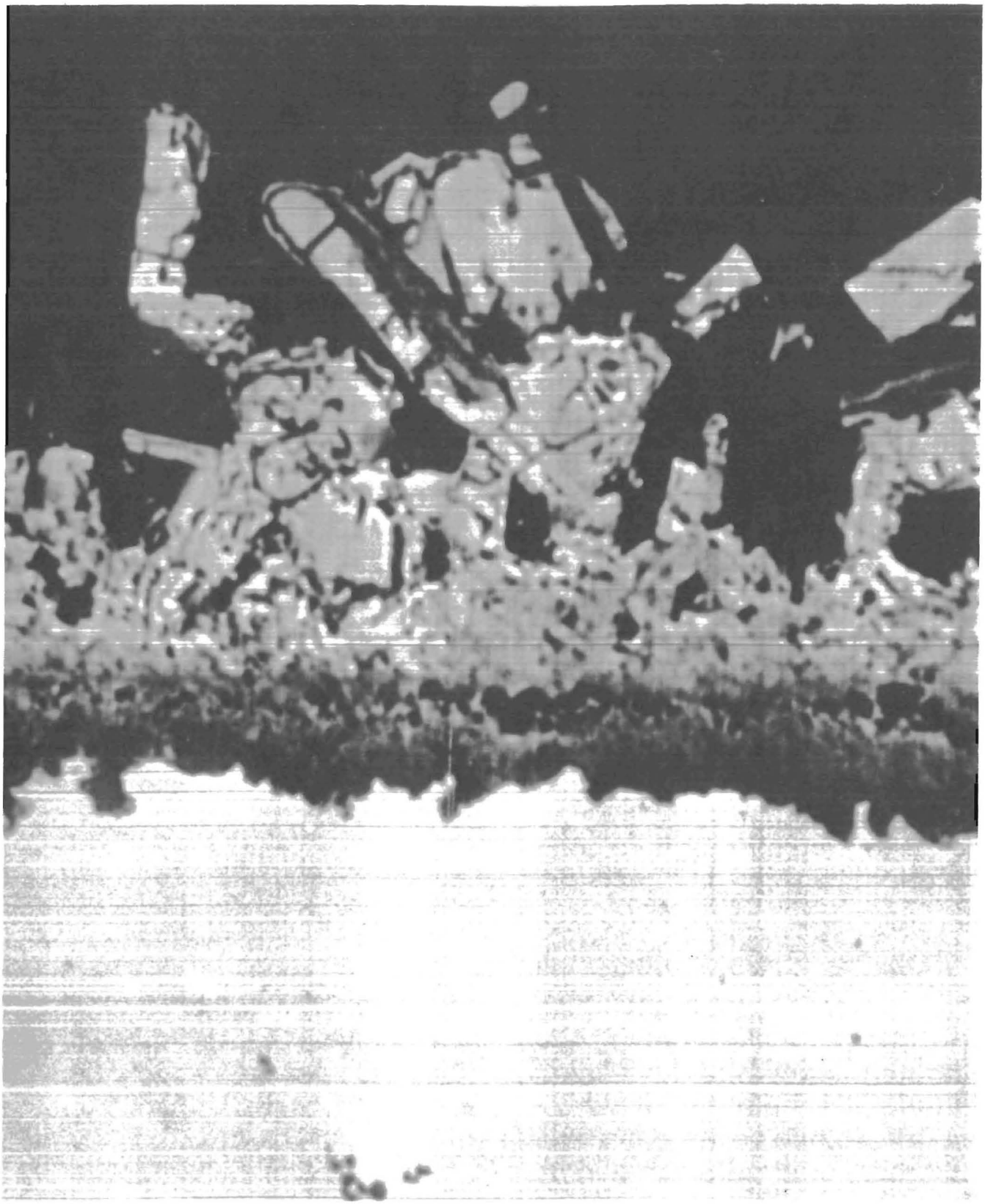

Figure 6.–Profiles of corrosion scales of alloys–alloy B (X 500).

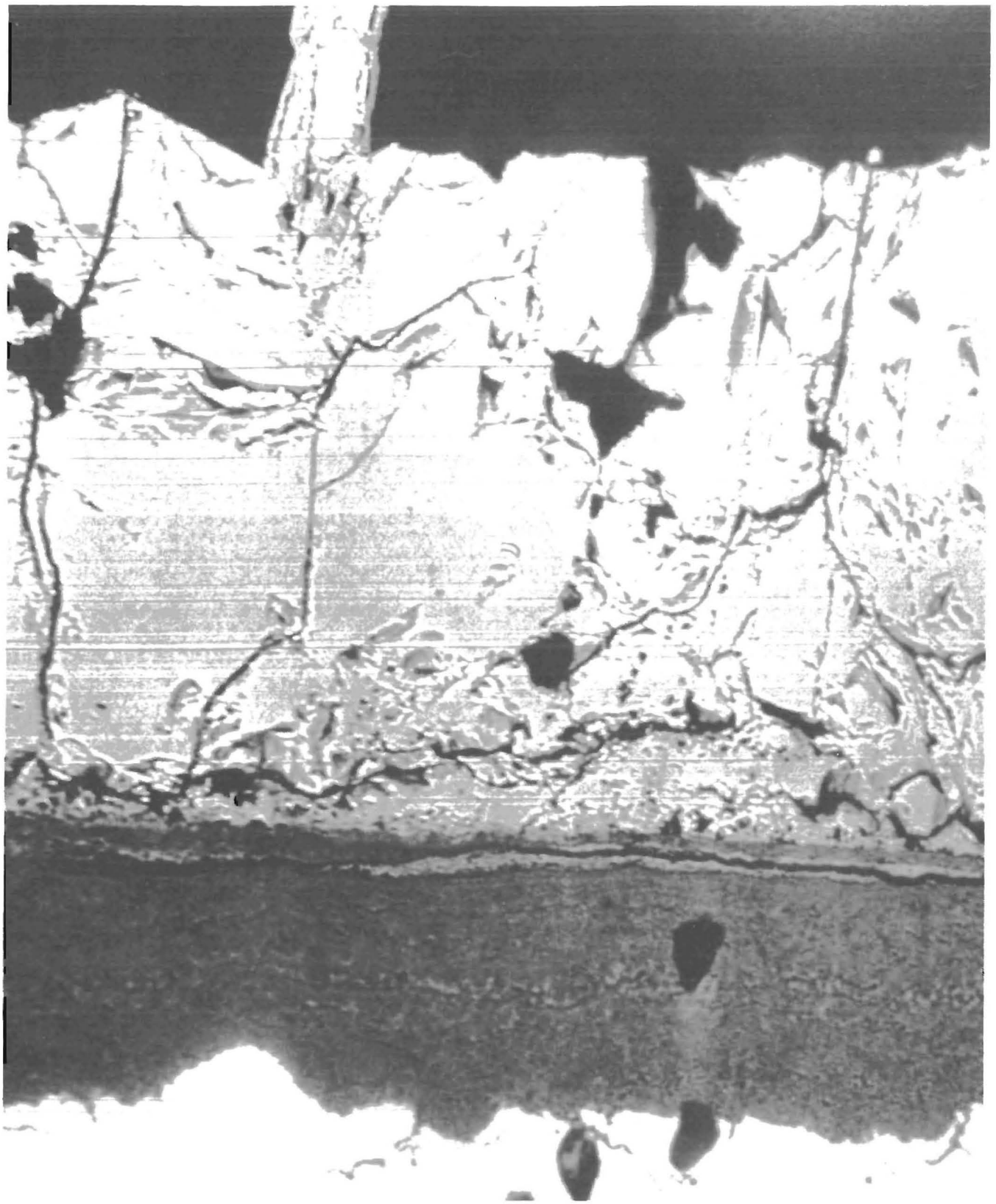

Figure 6.–Profiles of corrosion scales of alloys–alloy C (X 150).

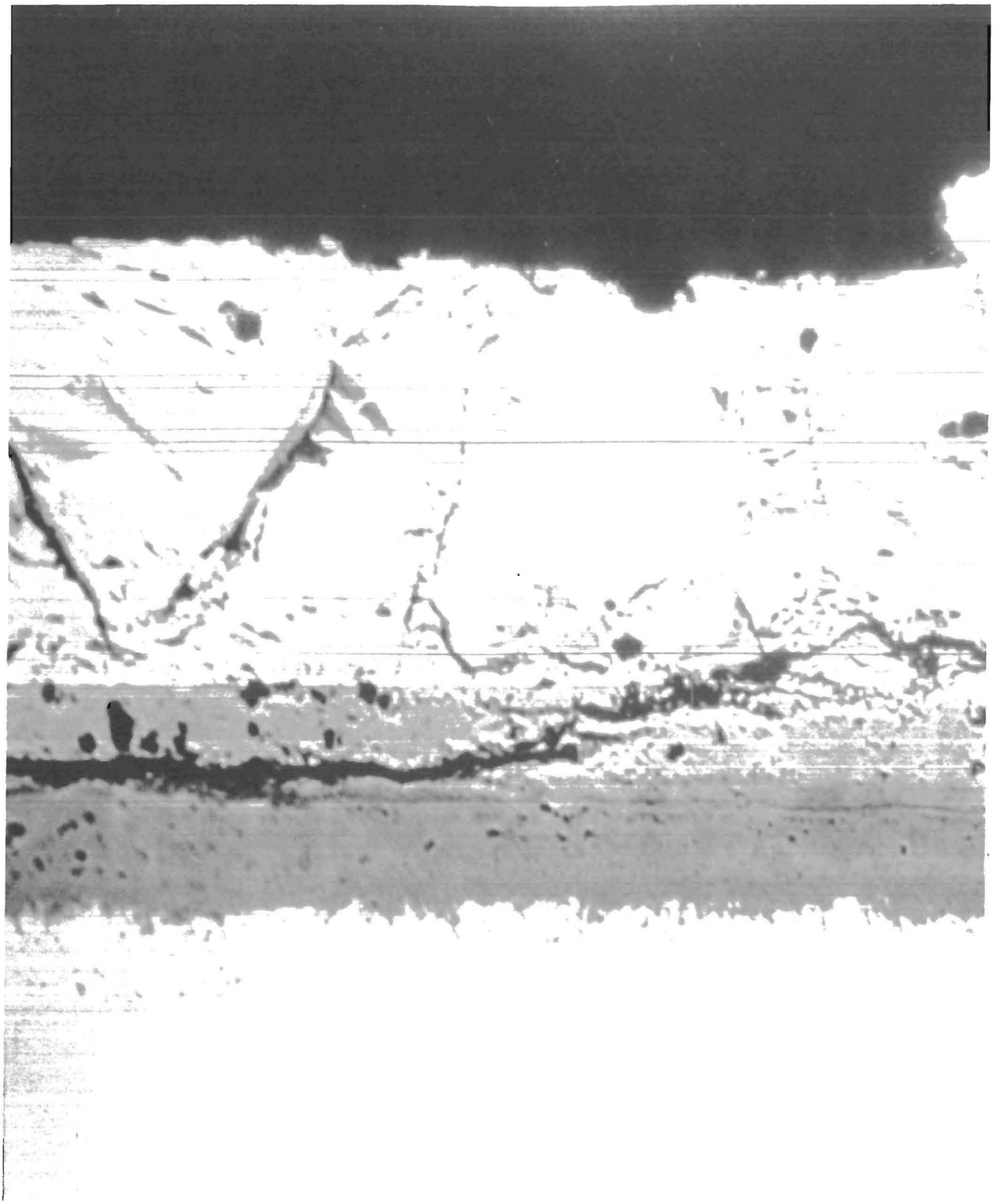

Figure 6.–Profiles of corrosion scales of alloys–alloy D (X 250).

ALUMINUM-CONTAINING ALLOYS–ALLOYS A AND B

An analysis of the scales indicated that Al plays a unique role in the corrosion mechanisms. In Al-containing alloys, three distinct layers were observed, while in alloys without Al, only two layers could be identified. An analysis of scales of Al-containing alloys is shown in tables 2 and 3.

Table 2.–Analysis of corrosion scale and base metal of alloy A near metal-scale interface, weight percent

Distance from interface, μm	Fe	Cr	Ni	Al	S	O
Corrosion scale:						
50 (outer)	50	9	2	0	37	2
15 (intermediate)	7	35	0	7	34	14
Approx 0 (inner)	13	32	1	17	18	15
Base metal:						
10	83	5	9.5	1.5	.5	.4
30	73	15.5	9	2.5	0	.3
50	71	18	9	2.5	0	0
100	71	18	8.5	2.5	0	0
Much greater than 100	68.7	18	9	4	0	0

Table 3.–Analysis of corrosion scale and base metal of alloy B near metal-scale interface, weight percent

Distance from interface, μm	Fe	Cr	Al	S	O
Corrosion scale:					
30 (outer)	59	6	0	33	2
20 (intermediate)	20	32	1.5	40	4
15 (intermediate)	30	22	8	19	19
Approx 0 (inner)	23	23	26	11	15
Base metal:					
10	87	11.5	1.5	0	0
30	79.5	18	2.5	0	0
100	79	18	2.5	0	0
Much greater than 100	76	19	4	0	0

In Al-containing alloys, the loosely packed, microcrystalline outer layer is made up essentially of FeS. The intermediate layer is an Fe-, Cr- and Al-containing mixed sulfide-oxide high in S. Both Cr and Al are concentrated in this layer, with Cr and S concentration increasing, and Al and O concentration decreasing outward through the intermediate layer. The inner layer in the scale in these alloys is tightly adherent, approximately 10 μm thick, with a very high Al concentration and high in O. Some S also is present, and there is some concentration of Cr, although the concentration is not as great as with Al. In alloy A, the concentration of Al is four times greater in the inner scale compared with a two times greater concentration for Cr; in alloy B, the concentration of Al is six times greater compared with one and one-third times greater concentration for Cr. This compares with a concentration approximately two times greater for both Cr and Al in the intermediate layers for both alloys A and B.

Other investigations (*5-8*) have determined that outward diffusion of the alloy components from the metal through the inner adherent layers of oxides and mixed sulfides determines the overall rate of scale growth. It is evident that in oxidizing S vapor environments (wet S vapor), a tightly adherent, mixed oxide-sulfide layer slows diffusion of Fe, Ni, Cr, and Al outward and slows the growth of the scale. Aluminum is largely held in the inner scale, while Cr diffuses through the inner scale and is also concentrated in the intermediate scale. The inner scale seems to prevent diffusion of Ni outward, and no depletion of Ni is observed in the base metal next to the metal-scale interface in alloy A. In alloy A, all layers of the scale are essentially devoid of Ni. As will be seen in the following section, this is in sharp contrast to alloys C and D. Chromium is depleted to a depth of 30 to 50 μm in both alloys A and B. Thus, the progress of corrosion can be represented by the model shown in figure 7 (top). Corrosion scale is multilayered, consisting of an outer porous layer of needles, blades, and plates of FeS_x. This outer layer is very loosely adherent and readily spalls during cooling of the specimen from temperature. An intermediate layer (Cr, Fe, Al) of sulfide is porous, and analysis indicates that S and O can penetrate through this layer toward the metal-scale interface. This intermediate layer also is loosely adherent and can be removed by brushing the surface of the corrosion specimens. Finally, a tightly adherent, high-Al, high-Cr (Al, Cr, Fe) oxide-sulfide layer, which limits the inward diffusion of S and O and the outward diffusion of Ni, is at the metal-scale interface. This innermost compact layer is approximately 15 μm in thickness and is not disrupted during the cooling of the specimen or by brushing the specimen surface.

The corrosion rate of Al-containing alloys is governed by the diffusion of Fe, Cr, or Al through the innermost compact layer. This is a reasonable assumption since, in the case of both oxidation and sulfidation of the common metals, oxide and sulfide scales grow primarily by outward diffusion of the cations rather than inward diffusion of O and/or S (*12*).

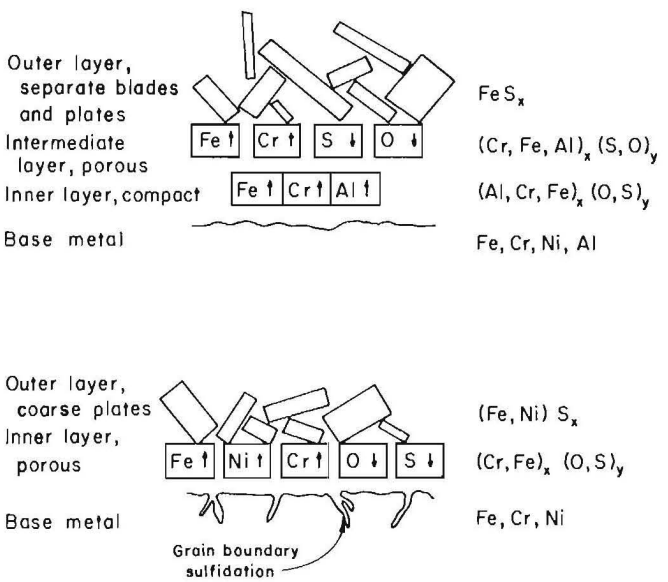

Figure 7.–Model of corrosion process in Al-containing alloys (top) and Al-free alloys (bottom).

ALUMINUM-FREE ALLOYS– ALLOYS C AND D

An analysis of scales for Al-free alloys is shown in tables 4 and 5. In alloys C and D, the Al-free alloys, a two-layer scale was observed rather than the three-layer scale observed in Al-containing alloys. The outer layer of alloy C was a very loosely adherent layer of coarse plates. The outer layer of alloy D was more uniform and compact on a macroscopic scale, with the exception of isolated massive, hexagonal crystals of FeS apparent on the surface.

Table 4.–Analysis of corrosion scale and base metal of alloy C near metal-scale interface, weight percent

Distance from interface, μm	Fe	Cr	Ni	S	O
Corrosion scale:					
125 (outer)	58	1	7	32	0.5
60 (outer)	46	5	7	32	2
15 (inner)	38	38	.5	10	13
Approx 0 (inner)	27	38	1	12	20
Base metal:					
10	73	17	9.5	1	2
Much greater than 100	73	18.2	9	0	0

Table 5.–Analysis of corrosion scale and base metal of alloy D near metal-scale interface, weight percent

Distance from interface, μm	Fe	Cr	Ni	S	O
Corrosion scale:					
85 (outer)	43	6	15	35	2
30 (outer)	40	7	15	32	5
20 (inner)	19	50	2	15	12
Approx 0 (inner)	8	67	1	4	18
Base metal:					
10	60	18	21	1.5	.5
Much greater than 100	54	28	19	0	0

As was the case with Al-containing alloys, the loosely packed outer layer was made up essentially of FeS with a minor Cr and, in this case, Ni presence. In the case of Al-containing alloys, outward diffusion of Ni was not observed, but in the Al-free alloys, concentrations of 7 wt pct (alloy C) and 15 wt pct (alloy D) Ni were observed in the outer scale. This was not true of the inner scale observed in both alloys C and D, which were essentially Ni free. This inner layer shared a heavy concentration of Cr, approximately two times the Cr content of the base metal in each case. While the inner layer was more compact and adherent than the outer FeS layer, it was not as adherent as the Al-containing scales and could be removed by vigorous brushing. The penetration of both O and S through the inner scale was evident in both EMPA and EDAX scans and was readily observed in the form of grain boundary attack in photomicrographs as illustrated in figure 3. The inner scale is 20 to 30 μm in thickness and high in O, with the O content increasing toward the metal-scale interface.

The corrosion of Al-free alloys can thus be represented by figure 7 (bottom). The model shows the two-layer scale, an outer layer of Fe-rich (Fe, Ni, Cr) $S_{(x)}$ and an inner layer of high Cr $(Cr, Fe)_x$ $(O, S)_y$. Grain boundary sulfidation and oxidation is observed. Rao (*14*) observed similar scales in Type 310 stainless steel and concluded that the outer layer was a single-phase sulfide scale made up of a solid solution of FeS-NiS-CrS. Rao also observed the relatively high Fe and Ni content and the low-Cr content of this outer layer.

DISCUSSION AND CONCLUSIONS

While the referenced literature indicates that Al additions can increase the corrosion resistance of Cr-containing steels to S environments, the dramatic increases in corrosion resistance observed in the study in oxidizing-S environments have not been previously reported. It is evident that if an S-containing environment can be adjusted by the injection of steam to an oxidizing environment, then the beneficial effects of Al additions to steel on sulfidation resistance can be greatly enhanced. Steam changes the S-containing environment from a reducing to an oxidizing environment. The greatly enhanced corrosion resistance of Al-containing alloys can be attributed to the formation and maintenance by diffusional processes of a thin, adherent, high-Al scale at the metal-scale interface. In these alloys, a three-layer scale is observed. The thin, high-Al protective scale is not observed in Al-free alloys, and a two-layer scale is observed. Corrosion in oxidizing-S atmospheres is reduced by a factor of 3 to 10 in Al-containing alloys. The protective, high-Cr, high-Al layer limits the inward diffusion of S and O and the outward diffusion of Ni at the metal-scale interface. The corrosion rate of Al-containing alloys is thus governed and rate limited by the diffusion of Fe, Cr, or Al through the innermost compact layer of a three-layer corrosion scale.

REFERENCES

1. Mrowec, S., and T. Werber. Mono Korozja Gazowa Metal (Gas Corrosion of Metals). Acad. Min. and Metall., Warsaw, Poland, TT76-54038, 1975, 528 pp. Engl. Transl., 1978, 561 pp., NTIS PB-283 054-T.

2. Corrosion Week. Aluminized Steel To Slow High-Sulfur Corrosion. V. 37, July 14, 1982, pp. 25-26.

3. McGill, W. A., and M. J. Weinbaum. Aluminum Diffused Steels Resist High Temperatures in Hydrocarbon Environments. Met. Prog., v. 115, No. 2, 1979, pp. 26-31.

4. Felten, E. High-Temperature Oxidation of Fe-Cr Base Alloys With Particular Reference to Fe-Cr-Y Alloys. J. Electrochem. Soc., v. 108, 1961, p. 450.

5. Golightly, F. A., F. H. Scott, and G. C. Wood. High-Temperature Corrosion of Fe-Cr-Al Alloys in Sulfur Vapor. Oxid. Met., v. 10, 1976, p. 163.

6. Kvernes, I., M. Oliveira, and P. Kofstad. High Temperature Oxidation of Fe-13Cr-XAl Alloys in Air/H_2O Vapor Mixtures. Corros. Sci., v. 17, 1977, p. 237.

7. Strafford, K. N., and R. Manifold. The Effects of Aluminum Alloying Additions on the Sulfidation Behavior of Iron. Oxid. Met., v. 5, 1972, p. 85.

8. Morrow, H., D. L. Sponseller, and E. Kalns. The Effects of Molybdenum and Aluminum on the Hot Corrosion (Sulfidation) Behavior of Experimental Nickel-Base Superalloys. Metall. Trans., v. 5, 1975, p. 673.

9. Mrowec, S., S. Tochowecz, T. Werber, and J. Podhorodecki. High Temperature Corrosion of Iron-Chromium-Aluminum Alloys. Corros. Sci., v. 7, 1967, p. 697.

10. Jallouli, E. M., J. P. Larpin, M. Lambertin, and J. C. Colson. Fe-Cr-Al, High Temperature Corrosion in Sulfur Vapor, J. Electrochem. Soc., v. 126, No. 12, 1979, p. 2254.

11. Oden, L. L., M. P. Krug, and R. A. McCune. Analysis of Vapor-Aluminum-Diffused Steels. BuMines RI 8629, 1982, 12 pp.

12. West, J. R. Austenitic Steels for Sulfur Vapor Service. Chem. Eng. (London), v. 58, 1951, p. 276.

13. Dunning, J. S. A Sulfidation-Oxidation-Resistant Ferritic Stainless Steel Containing Aluminum. BuMines RI 8856, 1984, 15 pp.

14. Rao, D. B., and H. G. Nelson. Sulfidation of 310 Stainless Steel at Sulfur Potentials Encountered in Coal Conversion Systems. Corros. Sci., v. 16, 1976, p. 464.

* U.S. GOVERNMENT PRINTING OFFICE: 611-012/00,122

INT.BU.OF MINES,PGH.,PA 29012